Journal of Drug Discovery and Health Sciences

journal home page : https://jddhs.com/index.php/jddhs/index

Research Article

Formulation, Optimization and Evaluation of Indigofera aspalathoides extract-loaded silver nanogel for wound healing applications: A QBD-based approach

Panchacharam G , Murali S , Velmurugan R *

Saveetha College of Pharmacy, Saveetha Institute of Medical and Technical Sciences, Chennai, India - 602105

ARTICLE INFO

Article history:
Received: 08 July, 2025
Revised: 12 August, 2025
Accepted: 05 September, 2025
Published: 25 Septembe, 2025

Keywords:
Qbd; Nanogel; Indigofera aspalathoides; carbopol; Wound healing; nanoparticle

DOI:
10.21590/jddhs.02.03.01

ABSTRACT

This study presents the formulation and optimization of a silver nanogel incorporating Indigofera aspalathoides extract (IAE) for potential wound healing applications. The nanogel was synthesized using the precipitation method, maintaining constant amounts of IAE and aqueous solution while varying the carbopol concentration (1–2% w/v) as the gelling agent. A Central Composite Rotatable Design was employed to optimize the formulation, followed by comprehensive physicochemical characterization. The nanogel's in vitro drug release profile, zeta potential, polydispersity index (PDI), particle size, viscosity, pH, homogeneity, and stability studies were conducted. The optimized formulation exhibited a yellowish-brown appearance, with a pH of 5.8 ± 0.2, viscosity of 9412 cP, and a particle size of 98 nm with a PDI of 0.204, indicating uniform dispersion. The zeta potential was measured at –22 mV, suggesting moderate stability. In vitro release studies showed a cumulative drug release of 86.28% over 8 hours and 98.06 % over 24 hrs. Scanning Electron Microscopy confirmed the spherical morphology of the nanoparticles. These results indicate that the IAE-loaded silver nanogel demonstrates favorable physicochemical properties and a controlled drug release profile, suggesting its potential as an effective topical delivery system for wound healing. Future studies should focus on in vivo evaluations, long-term stability, and clinical trials to further validate its therapeutic efficacy and safety.

Introduction

Herbal medicines form an indispensable component of traditional healthcare systems worldwide, particularly in Asian countries where Siddha and Ayurveda emphasize botanical preparations for chronic ailments such as inflammation, liver disorders, and skin diseases. In modern pharmacological research, many plant-derived bioactives have shown promising therapeutic potential, yet their direct clinical application remains restricted due to inherent limitations such as poor aqueous solubility, instability under physiological conditions, and limited systemic bioavailability (Kciuk et al., 2024; Singh, 2015). These challenges highlight the necessity for advanced drug delivery strategies that can enhance the pharmacokinetic and pharmacodynamic profiles of herbal constituents. In recent years, nanotechnology-based carriers have emerged as an effective solution to overcome such drawbacks (Parvin et al., 2025). Among these, nanogels—three-dimensional, hydrophilic polymeric networks in the nanometer size range—are gaining increasing attention.

***Corresponding Author:** R. Velmurugan,

Address: Saveetha Institute of Medical and Technical Sciences,Chennai, India.

Email ✉**:** ramaiyan.dr@gmail.com

Relevant conflicts of interest/financial disclosures: The authors declare that the research was conducted in the absence of any commercial or financial relationships that could be construed as a potential conflict of interest.

Nanogels possess a high water content, tunable swelling capacity, biocompatibility, and the ability to encapsulate both hydrophilic and hydrophobic molecules (Delgado-Pujol et al., 2025). Importantly, they enable controlled and sustained drug release, improved permeation across biological barriers, and protection of labile bioactives from degradation. Their versatility makes them particularly suited for topical and transdermal applications, where enhanced cutaneous penetration and retention are critical for therapeutic efficacy. Reports have shown that nanogel-based herbal formulations provide superior antioxidant and anti-inflammatory outcomes compared to conventional dosage forms, establishing them as a rational platform for plant-derived therapeutics (Kuthani et al., 2024; Ghosh et al., 2024).

One medicinal plant that stands out in this context is *Indigofera aspalathoides* (Vahl) DC, locally known as *Sivanar vembu* (Omprakash et al., 2013). Belonging to the family *Fabaceae*, it has a long history of use in Siddha medicine for the treatment of skin ailments (Gopalakrishnan et al., 2023), ulcers (Gupta et al., 2006), arthritis (Rajkapoor et al., 2009), liver diseases (Rajkapoor et al., 2006), and tumors (Ramya et al., 2021). Preclinical studies substantiate these claims: extracts of the plant have demonstrated anti-inflammatory (Bhagavan et al., 2013), antioxidant (Mahajan et al., 2016), hepatoprotective (Raman et al., 2025), antimicrobial (Kumar et al., 2018), and anticancer (Al-Saeedi & Rajendran, 2024) activities in various in vivo and in vitro models. The pharmacological activity of *I. aspalathoides* is largely attributed to its rich phytochemical profile, which includes Alkaloids, saponins, tannins, phenolic acids, flavonoids (Elangovan et al., 2014). For instance, a rhamnosylated flavone recently isolated from the plant exhibited significant anti-inflammatory activity in intestinal models, reinforcing the relevance of its flavonoid constituents (AlZahrani et al., 2024).

In addition to conventional phytochemical studies, *I. aspalathoides* has also been exploited for green nanotechnology applications, where its bioactive constituents act as natural reducing and stabilizing agents. An aqueous leaf extract was successfully used for the AgNPs biosynthesis in the size range of 20–50 nm, which demonstrated promising potential for wound-healing applications (Arunachalam et al., 2013). Similarly, a ZnO NPs was synthesised using the plant extract yielded crystalline nanoparticles with strong antioxidant activity, achieving nearly 98% free radical inhibition in the DPPH assay (Pragatheeswaran & Periakaruppan, 2025). More recently, selenium nanoparticles (SeNPs) prepared using ethanolic extracts of *I. aspalathoides* displayed potent antioxidant activity, along with significant cytoprotective and hepatoprotective effects against HepG2 liver cells, surpassing the activity of the crude extract alone (Raman et al., 2025). These findings highlight the plant's suitability as a green source for nanoparticle synthesis, providing enhanced biological activity through nanoscale delivery. Despite these advances, most of the reported nanostructures focus on metal or metal oxide nanoparticles, which are primarily investigated for antioxidant, antimicrobial, or anticancer properties.

However, challenges such as poor aqueous solubility, limited dermal penetration, and lack of controlled release of the phytoconstituents remain largely unaddressed. The formulation of such complex delivery systems requires more than empirical optimization. Application of QbD in nanogel formulation offers dual advantages: it ensures regulatory compliance while simultaneously improving product performance by systematically controlling variability. Therefore, the present study was undertaken to formulate and evaluate an *Indigofera aspalathoides* nanogel using QbD. By adopting a structured QbD framework, the study aimed to optimize formulation parameters, establish a robust design space, and comprehensively characterize the nanogel with respect to its physicochemical properties and therapeutic potential. This work not only addresses the limitations of conventional *I. aspalathoides* formulations but also contributes toward the advancement of evidence-based herbal nanomedicine.

Materials And Methods

Collection, Authentication and Preparation of Plant Extract

Fresh specimens of *Indigofera aspalathoides* were collected from the Tirunelveli District, Tamil Nadu, during the month of December. The plant was botanically identified and authenticated by experts at the Xavier Research Foundation, St. Xavier's College, Palayamkottai, Tamil Nadu. Healthy leaves were carefully selected, thoroughly cleaned, and shade-dried before being cut into small fragments. The dried material was pulverized into a fine powder using a mechanical grinder and stored in a desiccator until further use. Extraction was carried out using a Soxhlet apparatus with solvents of increasing polarity, including chloroform, ethanol, and water, to obtain different fractions of the crude extract for subsequent studies.

Preliminary Phytochemical Screening

Qualitative phytochemical screening was conducted on the extracts to identify key bioactive constituents (Table 1).

Formulation of Indigofera aspalathoides (IAE)-Incorporated Silver Nanogel

Synthesis of Silver Nanoparticles (AgNPs)

Silver nanoparticles were generated using a chemical reduction method supported by ultrasonication. Briefly, 125 mL of 0.002 M silver nitrate ($AgNO_3$) solution was heated to boiling. To this solution, 10 mL of 1% trisodium

Table 1: Preliminary phytochemical screening of I. aspalathoides extracts

Phytochemical Constituents	*Test Performed*	*Observation*
Alkaloids	Wagner's test (extract + Wagner's reagent)	Reddish-brown precipitate
Glycosides	Molisch test (α-naphthol in ethanol + conc. H_2SO_4)	Reddish-violet ring
Phenolic compounds	Ferric chloride test (extract + 5% $FeCl_3$)	Blue-green coloration
Tannins	Gelatin test (extract + 1% gelatin + 10% NaCl)	White precipitate
Flavonoids	Alkaline reagent test (extract + NaOH solution, then dilute HCl)	Yellow color turning colorless
Anthraquinones	Borntrager's test (extract + benzene + NH_4OH)	Pink to red coloration in ammoniacal layer
Sterols	Liebermann Burchard's (extract + acetic anhydride + conc. H_2SO_4)	Bluish green color
Terpenoids	Salkowski test (extract + chloroform + conc. H_2SO_4)	Red coloration in lower layer

citrate was introduced gradually under constant stirring. Ultrasonication was then performed with a Hielscher UP400S (400 W) at 90 °C for 15 minutes. The appearance of a pale-yellow coloration was taken as confirmation of nanoparticle formation. The prepared suspension was cooled to ambient temperature and stored in light-protected conditions until further use.

Preparation of IAE–Silver Nanogel

The nanogel base was developed by dispersing 0.75 g of carbopol 940 in 350 mL of double-distilled water. Subsequently, 100 mL of the synthesized AgNP suspension (50 ppm) and *Indigofera aspalathoides* extract (50 ppm) were incorporated into the dispersion, followed by ultrasonication for 400 seconds using the Hielscher system. Thereafter, 75 mL of trimethylamine was added slowly under continuous sonication to facilitate gelation. The process resulted in the formation of a stable, homogenous pale-yellow nanogel.

Optimization via Central Composite Rotatable Design

The formulation variables were optimized employing a Central Composite Rotatable Design (CCRD) using Design Expert® software (version 12). In this study, the key formulation parameters considered as independent variables were the concentration of silver nitrate (factor A), *Indigofera aspalathoides* extract (factor B), and carbopol 940 (factor C). Each factor was studied at three coded levels (−1, 0, +1). The responses selected for optimization included particle size (Y_1), zeta potential (Y_2), and polydispersity index (Y_3), as these parameters critically determine the stability and performance of nanodispersions. A total of 15 experimental runs were generated based on the design matrix (Tables 2). The experimental data were further analyzed through 3D response surface plots to interpret the interactive effects of the independent variables on the chosen responses. Optimization was performed with the goal of achieving minimum particle size, an optimal zeta potential value, and a low polydispersity index, thereby ensuring enhanced stability and uniformity of the nanogel system (Bharti et al., 2015; Velmurugan & Selvamuthukumar, 2016). The adequacy of the model was assessed by comparing predicted values with experimental observations, and the reliability of the optimization was confirmed by calculating the percentage bias.

Characterization of IAE-Loaded Silver Nanogel

Particle Size, Zeta Potential, and Polydispersity Index

The colloidal characteristics of the nanogel were assessed using dynamic light scattering (DLS) with a Malvern Zetasizer (ZEN 3000). These parameters were evaluated to determine particle size distribution, surface charge, and dispersion homogeneity, which are critical indicators of formulation stability (Kesharwani et al., 2020; Suryawanshi et al., 2025).

Scanning Electron Microscopy

The morphological attributes of the nanogel were examined using a scanning electron microscope (JSM 50A, Japan). Samples were mounted on aluminum stubs, sputter-coated, and observed at an accelerating voltage of 15 kV under a nitrogen atmosphere (10 °C/min). This analysis provided insights into particle shape and surface topology (Kesharwani et al., 2020; Suryawanshi et al., 2025).

Fourier-Transform Infrared Spectroscopy

FTIR spectra were recorded using a Thermo Scientific Nicolet iS50 spectrometer to identify characteristic

Table 2: Different independent variables and their levels used in CCRD for optimization of IAE loaded silver nanogel.

Independent variables	*Levels*		
	-1	0	+1
Silver nitrate conc. (mM)	3	5	7
Plant extract conc. (ml)	30	30	90
carbopol concentration (%W/V)	1	1.5	2

Table 3: Preliminary phytochemical analysis of I. aspalathoides extracts

S.No.	*Constituents*	*Aqueous Inference*	*Ethanol Inference*	*Chloroform Inference*
1	Alkaloids	+	+	+
2	Anthraquinones	-	+	-
3	Flavonoids	+	+	+
4	Glycosides	+	+	-
5	Phytosterol	+	-	-
6	Polyphenol	+	+	+
7	Tannins	-	+	-
8	Terpenoids	-	+	-
9	Sterols	+	-	+

'+' presence, '-' asbence

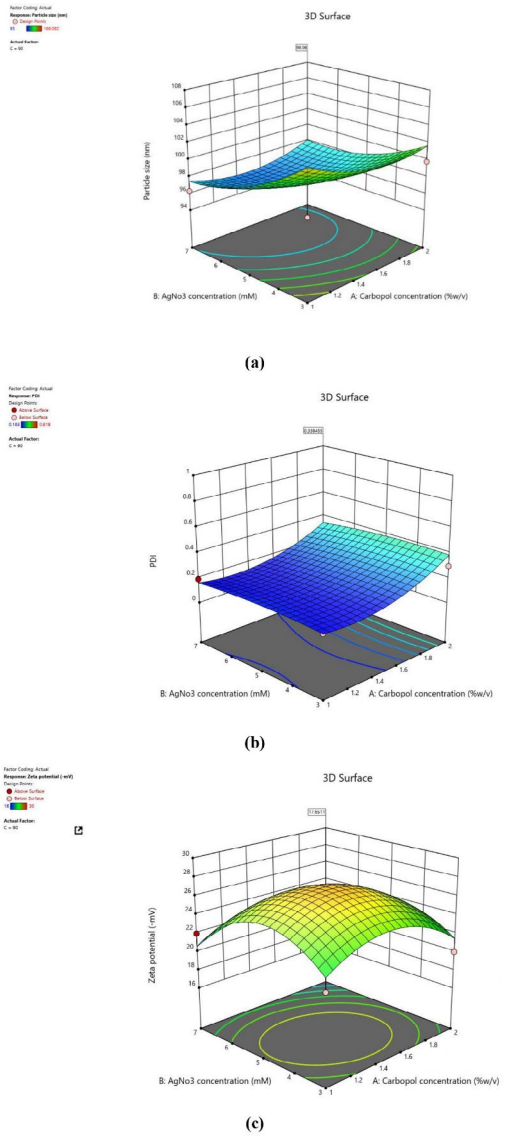

Figure 1: 3D response plot – showing the effect of independent variables on a) Particle size, (b) zeta potential and (c) polydispersity index

functional groups and evaluate possible molecular interactions between *Indigofera aspalathoides* extract and the silver nanogel matrix (Kesharwani et al., 2020; Suryawanshi et al., 2025).

Entrapment Efficiency

Entrapment efficiency was determined by ultracentrifugation. Briefly, 2 mL of the nanogel was diluted with ethanol and centrifuged at 2000 rpm for 20 min (Remi Instruments, India). The supernatant containing free drug was separated from the pellet, and the unencapsulated extract concentration was quantified at 352 nm using a UV–Visible spectrophotometer (UV3200, Lab India). EE (%) was calculated using the equation (Kesharwani et al., 2020; Suryawanshi et al., 2025):
Entrapment Efficiency (%) = Total IAE - Free IAE / Total IAE x 100

In Vitro Drug Release

The release profile of the formulation was studied using the dialysis bag diffusion technique. Equal volumes (20 mL) of the pure extract and the IAE-incorporated silver nanogel were loaded into dialysis membranes with a molecular weight cut-off of 10,000–12,000 Da and placed in 200 mL of phosphate buffer (pH 7.4) inside a USP type II dissolution apparatus. The setup was maintained at 37 ± 1 °C with continuous stirring at 100 rpm. At specific time intervals, 2 mL samples were withdrawn and replenished with fresh buffer to sustain sink conditions. The released IAE content was quantified by UV–visible spectrophotometry at 352 nm. Each experiment was performed in triplicate, and the collected samples were retained for subsequent stability analysis (Kesharwani et al., 2020; Suryawanshi et al., 2025).

Stability Studies

The optimized nanogel formulation was subjected to stability testing in accordance with ICH guidelines. Samples were packed in lacquered aluminum tubes and stored at three different conditions: refrigerated (4 ± 2 °C), room temperature (25 ± 2 °C), and accelerated (40 ± 2 °C)

Table 4: CCRD Matrix summarizing 15 experimental runs and their response

Std	*Run*	*Factor 1 A: carbopol Conc. (%w/v)*	*Factor 2 B: Silver Nitrate Conc(mM)*	*Factor 3 C: Plant Extract (ml)*	*Response 1 Particle size (nm)*	*Response 2 PDI*	*Response 3 Zeta Potential (mV)*
1	4	1	3	30	97.834	0.25	-20
2	20	2	3	30	98.995	0.209	-18
3	6	1	7	30	97.3365	0.213	-25
4	16	2	7	30	105.173	0.21	-22
5	13	1	3	90	98.6806	0.163	-21
6	15	2	3	90	99.7918	0.295	-20
7	5	1	7	90	96.3128	0.19	-22
8	1	2	7	90	96.2415	0.198	-18
9	8	0.659104	5	60	101.907	0.251	-23
10	3	2.3409	5	60	100.777	0.818	-21
11	7	1.5	1.63641	60	105.33	0.205	-22
12	12	1.5	8.36359	60	97.1381	0.201	-16
13	11	1.5	5	9.54622	101.209	0.21	-22
14	17	1.5	5	110.454	106.092	0.24	-23
15	2	1.5	5	60	95.1923	0.18	-30

for three months. At regular intervals, formulations were examined to assess their stability profile (Kesharwani et al., 2020; Suryawanshi et al., 2025).

Statistical Analysis

All results are presented as mean values accompanied by their standard deviations (SD). Statistical analyses were carried out using SPSS software (version 22.0, IBM Corp., Armonk, NY, USA). Group comparisons were assessed using the Student's t-test, and differences were regarded as statistically significant at $p < 0.05$.

Results & Discussion

Preliminary phytochemical analysis

The percentage yield of Indigofera aspalathoides extracts varied with the solvent used. The aqueous extract provided the maximum yield (14.31%), followed by ethanol (13.94%), while the chloroform extract showed the lowest recovery (11.05%). These findings indicate that water was the most efficient solvent for extracting bioactive constituents from the plant material.

The preliminary phytochemical analysis of *Indigofera aspalathoides* extracts revealed the presence of several bioactive constituents across the tested solvents (Table 3). The aqueous extract demonstrated presence of secondary metabolites, including alkaloids, flavonoids, glycosides, phytosterols, and polyphenols. Among these, flavonoids and polyphenols were strongly represented, indicating a phenolic-rich profile (Kumar et al., 2018). Tamilselvi et al., 2012 reported the phytochemical analysis of methanolic extracts of *Indigofera aspalathoides*, which showed the plant to be particularly rich in phenolic compounds (47.38±1.532 mg/g) compared to tannins (34.59±1.788 mg/g). This finding complements the ethanol and aqueous extract's phenolic-rich profile, suggesting that different solvents may extract varying amounts of phenolic compounds.

The ethanolic extract exhibited the presence of most major groups, particularly flavonoids, alkaloids, anthraquinones, polyphenols, terpenoids, tannins, terpenoids, and glycosides. This suggests that ethanol is the most suitable and effective solvent for extracting a broad range of bioactive phytoconstituents, particularly those with potential antioxidant properties. In support of this, Philips et al., 2010 evaluated the free radical scavenging activity of *Indigofera aspalathoides* leaf fractions and found that polyphenolic compounds were major contributors to antioxidant activity. The study revealed that both the chloroform and ethanolic fractions displayed significant antioxidant activity when compared to standard antioxidants. Interestingly, despite the chloroform fraction containing fewer polyphenolic compounds, it exhibited higher radical scavenging activity than the ethanolic fraction, indicating that the structural features of polyphenols may play a crucial role in their antioxidant potential. The chloroform extract, however, was limited mainly to alkaloids and sterols, which may provide additional pharmacological benefits but lacks the diversity of bioactive compounds seen in the aqueous and ethanolic extracts. Overall, the ethanolic extract exhibited the most comprehensive profile of bioactive phytoconstituents, making it the most suitable candidate for further formulation studies.

Optimization

Formulation optimization was carried out using CCRD with three independent variables (silver nitrate concentration, plant extract concentration, and carbopol concentration) and three responses (particle size, polydispersity index, and zeta potential) (Table 4).

Particle Size

The response surface analysis revealed that particle size was minimized (94–96 nm) at lower concentrations

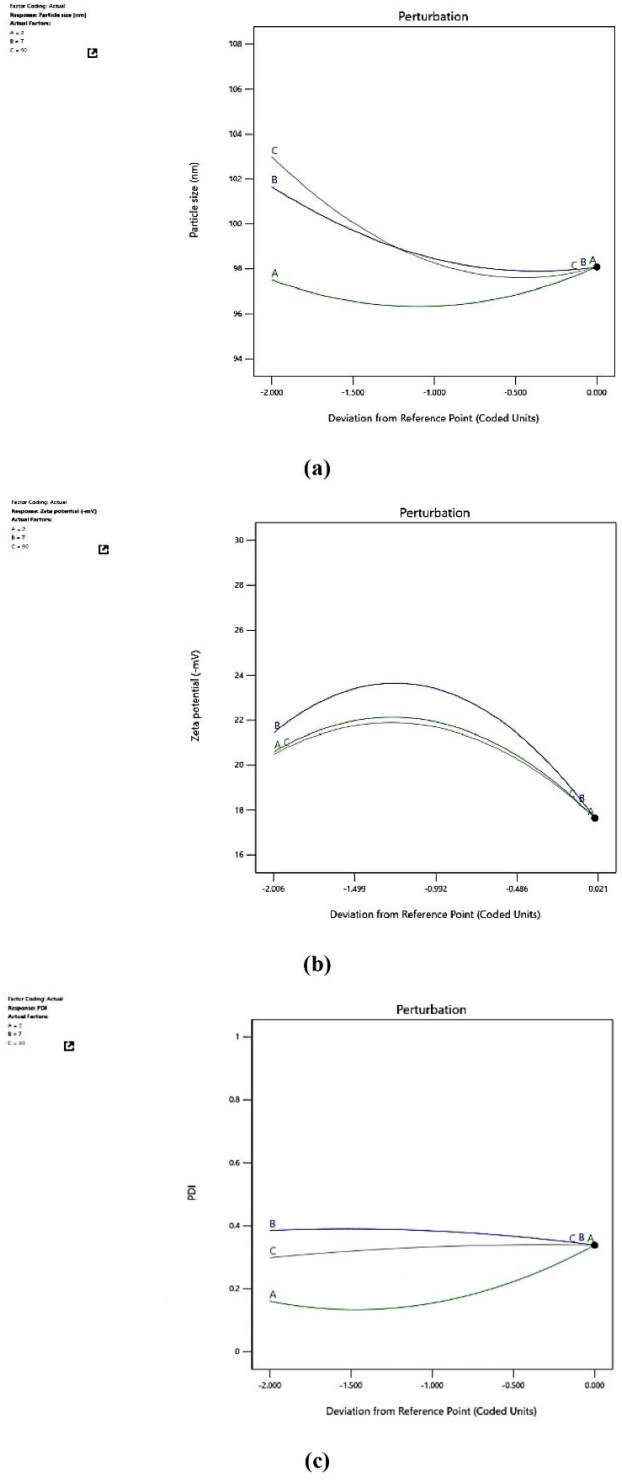

Figure 2: Perturbation plot showing the effect of each of the independent variables on (a) Particle size, (b) zeta potential and (c) polydispersity index, where A, B and C are carbopol concentration, silver nitrate concentration and plant extract concentration respectively

of both carbopol and $AgNO_3$ (Figure 1(a)). As carbopol concentration increased, a slight rise in particle size was observed, particularly at intermediate levels of $AgNO_3$. When both factors were simultaneously elevated, particle size increased further, reaching values around 105 nm. These findings suggest that while carbopol contributes to nanoparticle stabilization, excessive polymer content may promote aggregation or increase hydrodynamic diameter. Similar effects have been reported with other stabilizers such as PVP and PVA, where low-to-moderate concentrations effectively reduced particle size, but higher concentrations led to aggregation and larger diameters due to increased steric interactions (Higazy et al., 2021; Zein et al., 2022). Likewise, higher $AgNO_3$ concentrations favored particle growth and fusion of nuclei, consistent with previous observations that elevated silver precursor levels result in increased crystallite and particle dimensions (Gevorgyan et al., 2022). In green synthesis approaches using plant extracts, comparable trends have been observed, with nanoparticles typically ranging between 2–80 nm and strongly influenced by $AgNO_3$ concentration and stabilizer content (Liaqat et al., 2022). Thus, the optimal condition for achieving smaller nanoparticles lies at lower carbopol and moderate-to-low $AgNO_3$ concentrations. Importantly, the regression model for particle size was statistically significant ($p < 0.0001$) with an adjusted R^2 of 0.8126 and a low %CV of 3.28, indicating good predictive reliability of the model. Bias analysis showed differences between predicted and experimental values below 4%, confirming robustness of the particle size prediction. The perturbation plot for particle size demonstrated that factor B ($AgNO_3$ concentration) had the most pronounced effect, as indicated by the steep slope of its curve (Figure 2(a)). Increasing or decreasing $AgNO_3$ concentration caused significant deviations in particle size. In comparison, carbopol concentration and plant extract concentration showed flatter curves, signifying relatively smaller influences on particle size compared to $AgNO_3$.

PS = +147.54 - 13.38A + 0.5026B + 0.2197C + 5.62AB + 4.12AC - 22.13BC - 4.07A2 - 11.85B2 + 10.95C2

Polydispersity Index

The effect of formulation variables on the PDI showed a clear trend of decreasing PDI with increasing carbopol and $AgNO_3$ concentrations (Figure 1(b)). At low levels of both factors, the PDI was relatively high (0.3–0.4), indicating heterogeneity within the system. In contrast, higher concentrations of carbopol and $AgNO_3$ resulted in lower PDI values (<0.2), signifying a more uniform and monodisperse nanoparticle population. This outcome reflects the role of carbopol in preventing particle agglomeration and enhancing stability, while higher $AgNO_3$ concentrations ensure controlled and uniform nucleation. Similar findings have been reported in various studies,

Table 5: Assessment of Experimental and Predicted Parameters for Final Formulation

carbopol conc.	*AgNo3 Conc.*	*Plant extract conc.*	*Particle size*	*PDI*	*Zeta potential*
1.09	4.93	71.27			
Prediction			103	0.208	-22.63
Experimental			98	0.204	-22.24
Bias %			4.98%	1.92%	1.72%

Table 6: FTIR interpretation of IAE and IAE nanogel

Peak (cm^{-1})	*Sample*	*Functional Group*	*Interpretation*
3348.40	IAE	O-H Stretch	Broad peak indicating the presence of hydroxyl groups typical of phenolic compounds and alcohols in plant extracts (flavonoids, tannins).
1668.70	IAE	C=O Stretch	Characteristic of carbonyl compounds, likely from flavonoids or carboxylic acids in the plant extract.
1519.83	IAE	C=C Stretch	Indicates the presence of aromatic rings, typical of flavonoids and other polyphenolic compounds in the extract.
1213.34	IAE	C-O Stretch	Associated with ether or ester functional groups, confirming the presence of polyphenolic or flavonoid compounds in the extract.
3388.38	IAE nanogel	O-H Stretch	Shifted peak indicates interaction between hydroxyl groups from the plant extract and Cabopol, possibly due to hydrogen bonding.
1736.03	IAE nanogel	C=O Stretch	Suggests the incorporation of Cabopol (carboxylic acid groups) into the nanogel matrix, confirming polymer interaction.
1697.29	IAE nanogel	C=O Stretch	Further confirmation of Cabopol integration into the nanogel system through carbonyl stretching.
1023.28	IAE nanogel	C-O Stretch	Indicates the presence of C-O bonds in both the Cabopol polymer and Indigofera aspalathoides extract.
1453.50	IAE nanogel	C-H Bending	Confirms the interaction of aromatic rings and aliphatic chains in both the extract and polymer within the nanogel system.
1587.56	IAE nanogel	N-O Stretch	Indicates the presence AgNPs formed from $AgNO_3$ incorporation, confirming silver's interaction with the extract and polymer.

where carbopol was shown to improve nanoparticle uniformity by stabilizing the system. For instance, a study on PLGA nanoparticles loaded with luliconazole demonstrated that increasing carbopol concentrations (0.05% to 0.15% w/v) did not significantly affect particle size or PDI, suggesting its stabilizing role within this range (Chhajed et al., 2024). Moreover, the influence of $AgNO_3$ concentration on nanoparticle size distribution has been widely reported. A study on the green synthesis of silver nanoparticles using Galega officinalis extract found that higher concentrations of $AgNO_3$ led to smaller, more uniform nanoparticles, evidenced by a lower PDI, highlighting $AgNO_3$'s role in controlling nanoparticle size and uniformity (Manosalva et al., 2019).

Hence, the combination of elevated levels of both carbopol and $AgNO_3$ resulted in nanoparticles with a more consistent size distribution. Statistically, the regression equation for PDI showed the highest predictive accuracy, with an adjusted R^2 of 0.8563 and the lowest %CV (2.86), highlighting excellent reproducibility and reliability of the data. The adequate precision values greater than 10 further supported the robustness of the PDI model. The perturbation plot for PDI indicated that carbopol concentration had a greater impact compared to the other two factors (Figure 2(b)). This aligns with studies that reported the influence of carbopol on particle size distribution, where analysis revealed carbopol concentration as a key factor controlling PDI . The curve for factor A showed notable deviations, highlighting its strong influence on particle distribution and uniformity, while $AgNO_3$ concentration and plant extract concentration exhibited comparatively smaller effects on PDI, as reflected in their relatively flat curves. These results are consistent with research indicating that carbopol and

$AgNO_3$ concentrations play a critical role in modulating nanoparticle size and uniformity .

PDI= +0.2134 - 0.0009A - 0.0696B - 0.0012C + 0.0126AB - 0.02254AC + 0.0179BC - 0.0171A2 + 0.0844B2 - 0.0222C2

Zeta Potential

The zeta potential of the nanoparticles increased toward more positive values as carbopol and $AgNO_3$ concentrations were elevated, reaching peaks of approximately -28 to -30 mV (Figure 1(c)). At lower concentrations of both factors, the zeta potential dropped to -15 to -18 mV, suggesting reduced colloidal stability. Moderate-to-higher ranges of both variables enhanced electrostatic stability, as indicated by zeta potential values exceeding -25 mV, which are generally considered optimal for preventing aggregation. The observed trend highlights the contribution of carbopol's charged functional groups to the surface charge of nanoparticles, while increased $AgNO_3$ concentration supports ionic balance and charge stabilization (Badawy et al., 2010). Together, these factors improved colloidal stability through enhanced electrostatic repulsion. Consistent with this, the zeta potential regression model was statistically significant ($p < 0.0001$), with an adjusted R^2 of 0.8090 and %CV of 3.89, demonstrating acceptable accuracy. Bias values remained within 4% of experimental observations, confirming the model's predictive strength. The perturbation plot for zeta potential showed that $AgNO_3$ concentration was the dominant contributor to variations in zeta potential values (Figure 2(c)). The curve for factor B displayed a marked rise and fall, indicating strong sensitivity of surface charge stability to $AgNO_3$ concentration. In contrast, factor A and factor C produced minimal shifts compared to factor B.

ZP = +22.98 - 0.0965A + 0.9818B + 0.4427C + 0.0750AB - 0.3750AC + 1.12BC - 0.0592A2 - 1.48B2 - 0.0192C2

Model Validation: Comparison of Predicted and Observed Values

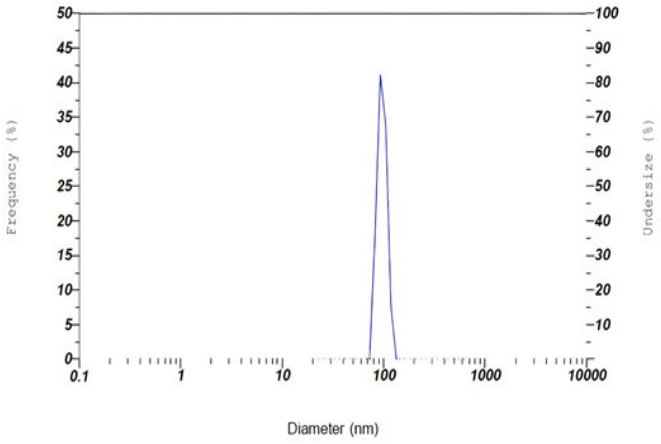

Figure 3: Particle size distribution of IAE loaded silver nanogel

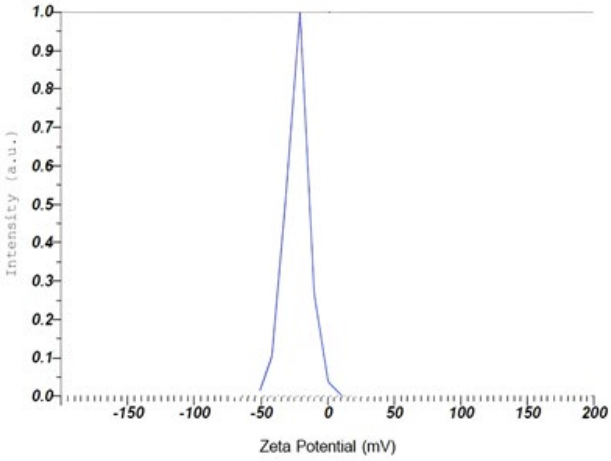

Figure 4: Zeta potential distribution of IAE loaded silver nanogel

The optimized formulation was obtained at carbopol concentration of 1.09%, $AgNO_3$ concentration of 4.93 mM, and plant extract concentration of 71.27 µg/mL. Under these conditions, the Design-Expert model predicted a particle size of 156 nm, PDI of 0.208, and zeta potential of -22.63 mV. Experimental validation of the optimized batch yielded a particle size of 148 nm, PDI of 0.204, and zeta potential of -22.24 mV.

The calculated bias between predicted and experimental values was 4.98% for particle size, 1.92% for PDI, and 1.72% for zeta potential. All values were within the predefined acceptance criteria of 6%, indicating excellent agreement between model predictions and experimental outcomes (Table 5). This validates the robustness and reliability of the optimization process, confirming that the applied response surface methodology can effectively predict nanoparticle characteristics under defined formulation conditions.

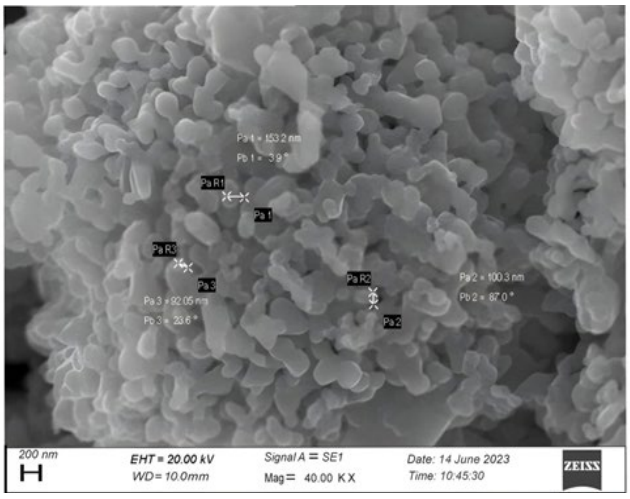

Figure 5: SEM image of IAE loaded silver nanogel.

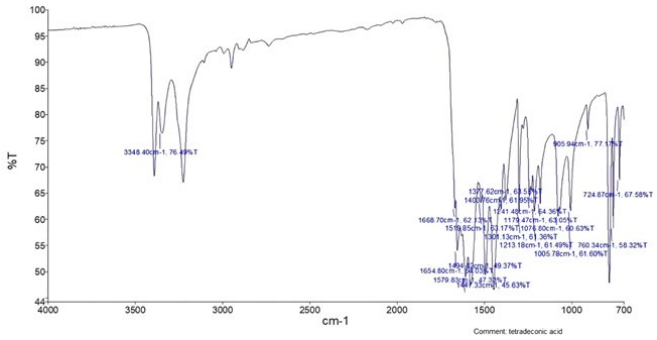

Figure 6(a) : FTIR spectroscopic profile of IAE.

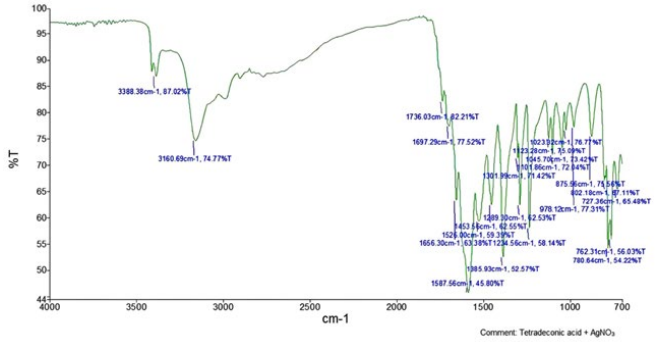

Figure 6(b) : FTIR spectroscopic profile of IAE loaded silver nano gel

Characterization of IAE loaded silver nanogel formulation

Dynamic Light Scattering

The average particle size was 98 nm (Figure 3) with a zeta potential of -22 mV (Figure 4), indicating high stability and effective colloidal dispersion. Particle size distribution curve reveals that the nanogel obtained were polydisperse in nature. The high magnitude of negative zeta potential indicates strong electrostatic repulsion between particles, which contributes to enhanced colloidal stability, uniform dispersion, and prolonged shelf life of the nanoparticles (Pochapski et al., 2021).

SEM analysis

The SEM analysis reveals a porous and granular surface morphology characteristic of polymer-based nanogels, with aggregated nanoparticles forming a crosslinked network (Figure 5). The particle size distribution, as indicated by the measurements Pa1, Pa2, and Pa3, shows nanoparticles ranging from approximately 92 nm to 153.2 nm, suggesting that the nanogel consists of small, well-distributed particles. Additionally, the angular measurements (Pb1, Pb2, Pb3) indicate the orientations of the nanoparticle clusters, with angles around 23.6°, 3.9°, and 87.0°, which may reflect the structural alignment of the nanoparticles within the gel network. This data provides insight into the mechanical properties and interaction of the nanogel with its surrounding environment, particularly in applications like drug delivery, where the nanoparticle alignment and size can influence performance.

FTIR analysis

The spectrum revealed several notable peaks that correspond to the functional groups in the *Indigofera aspalathoides* extract and the nanogel (Table 6) (Figure 6 (a) & (Figure 6 (b)).

Entrapment efficiency

The EE of the *Indigofera aspalathoides* extract in the silver nanogel formulation was found to be 85%, indicating that a significant portion of the IAE was successfully encapsulated within the nanogel matrix. This suggests the formulation's effectiveness in retaining the active compounds for controlled release.

In-vitro drug release

The in vitro release behavior of IAE was evaluated by comparing the pure extract with the silver nanogel formulation (Figure 7). Pure IAE demonstrated a rapid release pattern, with almost complete release occurring within 8 hours, reflecting its fast-releasing nature. On the other hand, the nanogel system displayed a more gradual and sustained release, where about 86.28% of the drug was released within 8 hours, progressively increasing to 98.06% at 24 hours. This extended release can be attributed to the entrapment of IAE within the nanogel matrix, which acts as a barrier to immediate diffusion. The findings confirm that the IAE-loaded silver nanogel is capable of providing prolonged and controlled drug release, thereby offering the advantage of sustained therapeutic action.

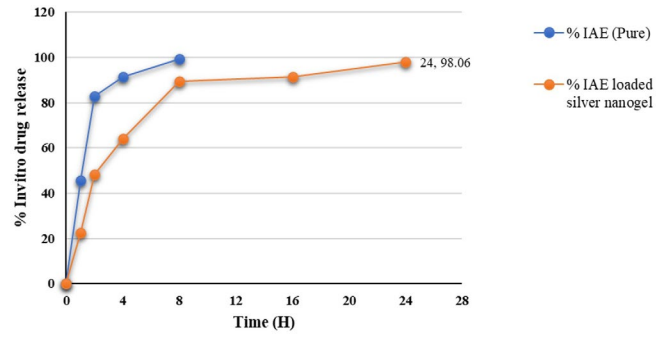

Figure 7: Cumulative Invitro drug release of IAE and IAE loaded silver nanogel

Stability studies

The stability of the IAE-loaded silver nanogel formulation was assessed over a three-month period at 4 ± 2°C, 25 ± 2°C, and 40 ± 2°C. At 4 ± 2°C, the formulation exhibited

excellent stability, with no degradation observed throughout the study. The pH remained consistent at 5.8, and the viscosity showed minimal variation, ranging from 9412.15 cP to 9387.08 cP, indicating that the low temperature effectively preserved the formulation. At 25 ± 2°C, the formulation maintained good stability, with only 1% degradation by the third month. The pH remained stable at 5.8, and the viscosity slightly decreased from 9412.15 cP to 9326 cP, suggesting that room temperature had a minimal impact on the formulation's properties. However, at 40 ± 2°C, the formulation experienced 6% degradation by the third month, accompanied by a slight decrease in pH (from 5.8 to 5.1) and a noticeable reduction in viscosity (from 9412.15 cP to 9134.70 cP), indicating accelerated degradation. These results suggest that the formulation is most stable when stored at 4 ± 2°C, with minimal degradation and consistent pH and viscosity, while 40 ± 2°C should be avoided for long-term storage.

CONCLUSION

The study successfully developed and optimized a silver nanogel containing *Indigofera aspalathoides* extract using Central Composite Rotatable Design. The optimized formulation exhibited favorable physicochemical characteristics, including suitable pH, viscosity, nanosized particles with uniform distribution, and good stability. In vitro drug release studies demonstrated a controlled and sustained release profile, while SEM analysis revealed well-defined spherical morphology of the nanoparticles. Overall, these results suggest that the IAE-loaded silver nanogel holds significant promise as a topical delivery system for wound healing applications. However, comprehensive in vivo studies, extended stability testing, and clinical validation are necessary to confirm its therapeutic effectiveness and safety under practical conditions..

Acknowledgement

The authors sincerely thank Saveetha College of Pharmacy, SIMATS for providing the necessary facilities, resources, and support to carry out this research successfully.

Declaration of Interest

The authors declare that they have no known competing financial interests or personal relationships that could have appeared to influence the work reported in this paper.

Funding Statement

This research received no external funding.

Data Availability

The data supporting the findings of this study are available from the corresponding author upon reasonable request.

REFERENCES

1. Al-Saeedi, F. & Rajendran, P., (2024). Anti-metastasis activity of 5,4'-dihydroxy 6,8-dimethoxy 7-O-rhamnosyl flavone from *Indigofera aspalathoides* Vahl on breast cancer cells. Scientific Reports, 14(1):12349. https://doi.org/10.1038/s41598-024-63136-2
2. AlZahrani, A.M., Rajendran, P., Bekhet, G.M., Balasubramanian, R., Govindaram, L.K., Ahmed, E.A. & Hanieh, H., (2024). Protective effect of 5,4'-dihydroxy-6,8-dimethoxy-7-O-rhamnosylflavone from *Indigofera aspalathoides* Vahl on lipopolysaccharide-induced intestinal injury in mice. Inflammopharmacology, 32(5):3537–3551. https://doi.org/10.1007/s10787-024-01530-y
3. Arunachalam, K.D., Annamalai, S.K., Arunachalam, A.M. & Kennedy, S., (2013). Green synthesis of crystalline silver nanoparticles using *Indigofera aspalathoides*—Medicinal plant extract for wound healing applications. Asian Journal of Chemistry, 25:1–8.
4. Badawy, A.M., Luxton, T.P., Silva, R.G., Scheckel, K.G., Suidan, M.T. & Tolaymat, T.M., (2010). Impact of environmental conditions (pH, ionic strength, and electrolyte type) on the surface charge and aggregation of silver nanoparticles suspensions. Environmental Science & Technology, 44(4):1260–1266. https://doi.org/10.1021/es902240k
5. Bhagavan, N.B., Arunachalam, S. & Dhasarathan, P., (2013). Evaluation of anti-inflammatory activity of *Indigofera aspalathoides* Vahl in Swiss albino mice. Journal of Pharmacy Research, 6(3):350–354. https://doi.org/10.1016/j.jopr.2013.02.018
6. Bharti, C., Nagaich, U., Pal, A.K. & Gulati, N., (2015). Mesoporous silica nanoparticles in target drug delivery system: A review. International Journal of Pharmaceutical Investigation, 5(3):124–133. https://doi.org/10.4103/2230-973X.160844
7. Chhajed, S.S., Laddha, U.D., Sonawane, S.S., Pekhale, M., Thorat, P., Kshirsagar, S.J. & Sangshetti, J.N., (2024). Formulation, development and characterization of PLGA-luliconazole nanoparticles loaded gel system for topical fungal treatment. Indian Journal of Pharmaceutical Education and Research, 58(1s):s187–s195. https://archives.ijper.org/sites/default/files/IndJPhaEdRes-58-1s-187.pdf
8. Delgado-Pujol, E.J., Martínez, G., Casado-Jurado, D., Vázquez, J., León-Barberena, J., Rodríguez-Lucena, D., Torres, Y., Alcudia, A. & Begines, B., (2025). Hydrogels and nanogels: Pioneering the future of advanced drug delivery systems. Pharmaceutics, 17(2):215. https://doi.org/10.3390/pharmaceutics17020215
9. Elangovan, K., Thanigaivel, S., Shahinbanu, Z. & Murugesan, K., (2014). Phytochemical evaluation, in vitro antioxidant and antibacterial potential of *Indigofera aspalathoides*. International Journal of Pharmacy and Biological Sciences, 4(1):161–168. https://ijpbs.com/ijpbsadmin/upload/ijpbs_53462923dfd5b.pdf
10. Gevorgyan, S., Schubert, R., Falke, S., Lorenzen, K., Trchounian, K. & Betzel, C., (2022). Structural characterization and antibacterial activity of silver nanoparticles synthesized using a low-molecular-weight royal jelly extract. Scientific Reports, 12(1):14077. https://doi.org/10.1038/s41598-022-17929-y
11. Ghosh, A., Majie, A. & Gorain, B., (2024). Nanobiomaterials in the management of wound healing. In: Biomaterial-Inspired Nanomedicines for Targeted Therapies, Springer, Singapore, 277–304. https://doi.org/10.1007/978-981-97-3925-7_10
12. Gopalakrishnan, A.V., Krishnan, N., Singh, P.K., Velmurugan, D., Kandasamy, R. & Pachaiappan, R., (2023). Analysis of the secondary metabolites of *Indigofera aspalathoides* DC oil to control various human ailments. In: Therapeutic Protein Targets for Drug Discovery and Clinical Evaluation: Bio-Crystallography and Drug Design, 339–384. https://doi.org/10.1142/9789811254796_0012
13. Gupta, M., Mazumder, U.K., Haldar, P.K., Kander, C.C., Manikandan, L. & Senthilkumar, G.P., (2006). Protective effect of *Indigofera aspalathoides* in chemical induced gastric mucosal lesions in rats. Oriental Pharmacy and Experimental Medicine, 6(1):53–57. https://www.dbpia.co.kr/Journal/articleDetail?nodeId=NODE09869694

14. Higazy, I.M., Mahmoud, A.A., Ghorab, M.M. & Ammar, H.O., (2021). Development and evaluation of polyvinyl alcohol stabilized polylactide-co-caprolactone-based nanoparticles for brain delivery. Journal of Drug Delivery Science and Technology, 61:102274. https://doi.org/10.1016/j.jddst.2020.102274
15. Kciuk, M., Garg, A., Rohilla, M., Chaudhary, R., Dhankhar, S., Dhiman, S., Bansal, S., Saini, M., Singh, T.G., Chauhan, S. & Mujwar, S., (2024). Therapeutic potential of plant-derived compounds and plant extracts in rheumatoid arthritis—Comprehensive review. Antioxidants, 13(7):775. https://doi.org/10.3390/antiox13070775
16. Kesharwani, P., Jain, A., Srivastava, A.K. & Keshari, M.K., (2020). Systematic development and characterization of curcumin-loaded nanogel for topical application. Drug Development and Industrial Pharmacy, 46(9):1443–1457. https://doi.org/10.1080/03639045.2020.1793998
17. Kumar, T.T., Salique, S.M., Ilyas, M.H., Thajuddin, N., Panneerselvam, A., Padusha, M.K. & Jahangir, H.S., (2018). Phytochemical screening and antimicrobial studies in leaf extracts of *Indigofera aspalathoides* (Vahl.). Pharmacognosy Journal, 10(6):1208-1215. http://dx.doi.org/10.5530/pj.2018.6.207
18. Kuthani, A., Kommu, S., Banoth, S.K., Manda, R.M., Pathakala, N. & Boggula, N., (2024). Nanotechnology in herbal medicine: New perspectives and challenges. In: Techniques and Innovative Research in Pharmaceutical Science, 109-143.
19. Liaqat, N., Jahan, N., Anwar, T. & Qureshi, H., (2022). Green synthesized silver nanoparticles: Optimization, characterization, antimicrobial activity, and cytotoxicity study by hemolysis assay. Frontiers in Chemistry, 10:952006. https://doi.org/10.3389/fchem.2022.952006
20. Mahajan, P., Gnana Oli, R., Jachak, S.M., Bharate, S.B. & Chaudhuri, B., (2016). Antioxidant and antiproliferative activity of indigocarpan, a pterocarpan from *Indigofera aspalathoides*. Journal of Pharmacy and Pharmacology, 68(10):1331–1339. https://doi.org/10.1111/jphp.12609
21. Manosalva, N., Tortella, G., Diez, M.C., Schalchli, H., Seabra, A.B., Durán, N. & Rubilar, O., (2019). Green synthesis of silver nanoparticles: Effect of synthesis reaction parameters on antimicrobial activity. World Journal of Microbiology and Biotechnology, 35(6):88. https://doi.org/10.1007/s11274-019-2664-3
22. Omprakash, K.K., Chandran, G.S. & Velpandian, V., (2013). *Indigofera aspalathoides* Vahl ex. DC. (Sivanar Vembu): A phyto-pharmacological review. International Journal of Pharmaceutical Sciences and Research, 4(10):3775. http://dx.doi.org/10.13040/IJPSR.0975-8232.4(10).3775-81
23. Parvin, N., Aslam, M., Joo, S.W. & Mandal, T.K., (2025). Nano-phytomedicine: Harnessing plant-derived phytochemicals in nanocarriers for targeted human health applications. Molecules, 30(15):3177. https://doi.org/10.3390/molecules30153177
24. Philips, A., Philip, S., Arul, V., Padmakeerthiga, B., Renju, V., Santha, S. & Sethupathy, S., (2010). Free radical scavenging activity of leaf extracts of *Indigofera aspalathoides*—An in vitro analysis. Journal of Pharmaceutical Sciences and Research, 2(6):322–328.
25. Pochapski, D.J., Carvalho dos Santos, C., Leite, G.W., Pulcinelli, S.H. & Santilli, C.V., (2021). Zeta potential and colloidal stability predictions for inorganic nanoparticle dispersions: Effects of experimental conditions and electrokinetic models on the interpretation of results. Langmuir, 37(45):13379–13389. https://doi.org/10.1021/acs.langmuir.1c02056
26. Pragatheeswaran, N.S. & Periakaruppan, R., (2025). Bio-synthesis of zinc oxide nanoparticles with antioxidant potential using *Indigofera aspalathoides* via green chemistry approach. Biomedical Materials & Devices, 1–9. https://doi.org/10.1007/s44174-025-00463-6
27. Rajkapoor, B., Jayakar, B., Kavimani, S. & Murugesh, N., (2006). Protective effect of *Indigofera aspalathoides* against CCl4-induced hepatic damage in rats. Journal of Herbal Pharmacotherapy, 6(1):49–54. https://doi.org/10.1080/J157v06n01_05
28. Rajkapoor, B., Kavimani, S., Ravichandiran, V., Sekhar, K., Kumar, R.S., Kumar, M.R., Pradeepkumar, M., Einstein, J.W., Kumar, E.P., (2009). Effect of *Indigofera aspalathoides* on complete Freund's adjuvant-induced arthritis in rats. Pharmaceutical Biology, 47(6):553–557. https://doi.org/10.1080/13880200902902489
29. Raman, S., Kasirajan, S., Chinnapandi, B., Karthikeyan, K., Pandian, A., Chandrasekaran, K., Al-Ansari, M.M., Sugumar, V. & Srinivasan, P., (2025). Luminescent biogenic selenium nanoparticles from *Indigofera aspalathoides* Vahl ex DC: A novel hepatoprotective strategy for enhancing liver health. Luminescence, 40(2):e70101. https://doi.org/10.1002/bio.70101
30. Raman, S., Kasirajan, S., Chinnapandi, B., Karthikeyan, K., Pandian, A., Chandrasekaran, K., Al-Ansari, M.M., Sugumar, V. & Srinivasan, P., (2025). Luminescent biogenic selenium nanoparticles from *Indigofera aspalathoides* Vahl ex DC: A novel hepatoprotective strategy for enhancing liver health. *Luminescence*, 40(2):e70101. https://doi.org/10.1002/bio.70101
31. Ramya, V., Madhu-Bala, V., Prakash-Shyam, K., Gowdhami, B., Sathiya-Priya, K., Vignesh, K., Vani, B. & Kadalmani, B., (2021). Cytotoxic activity of *Indigofera aspalathoides* (Vahl.) extracts in cervical cancer (HeLa) cells: Ascorbic acid adjuvant treatment enhances the activity. Phytomedicine Plus, 1(4):100142. https://doi.org/10.1016/j.phyplu.2021.100142
32. Singh, D., (2015). Application of novel drug delivery system in enhancing the therapeutic potential of phytoconstituents. Asian Journal of Pharmaceutics (AJP), 9(4):1-12. https://doi.org/10.22377/ajp.v9i4.480
33. Suryawanshi, N.R., Nagoba, S.N., Agarkar, P., Chavan, R., Patil, R., Mehtre, P. & Dhanve, N., (2025). Design, development and evaluation of herbal nanogel containing *Achyranthes aspera*. Research Journal of Pharmacy and Technology, 18(7):2961–2966. https://doi.org/10.52711/0974-360X.2025.00424
34. Tamilselvi, N., Krishnamoorthy, P., Dhamotharan, R., Arumugam, P. & Sagadevan, E., (2012). Analysis of total phenols, total tannins and screening of phytocomponents in *Indigofera aspalathoides* (Shivanar Vembu) Vahl ex DC. Journal of Chemical and Pharmaceutical Research, 4(6):3259–3262.
35. Velmurugan, R. & Selvamuthukumar, S., (2016). Development and optimization of ifosfamide nanostructured lipid carriers for oral delivery using response surface methodology. Applied Nanoscience, 6:159–173. https://doi.org/10.1007/s13204-015-0434-6
36. Zein, R., Alghoraibi, I., Soukkarieh, C., Ismail, M.T. & Alahmad, A., (2022). Influence of polyvinylpyrrolidone concentration on properties and antibacterial activity of green synthesized silver nanoparticles. Micromachines, 13(5):777. https://doi.org/10.3390/mi13050777

HOW TO CITE THIS ARTICLE: Panchacharam, G., Murali, S., Velmurugan, R. Formulation, Optimization and Evaluation of Indigofera aspalathoides extract-loaded silver nanogel for wound healing applications: A QBD-based approach. J. of Drug Disc. and Health Sci. 2025;2(3):1-11. **DOI:** 10.21590/jddhs.02.03.01